



Colloidal surface interactions and membrane fouling: Investigations at pore scale

P. Bacchin^{a,b,*}, A. Marty^{a,b}, P. Duru^{c,d}, M. Meireles^{a,b}, P. Aimar^{a,b}

^a Université de Toulouse, INPT, UPS, Laboratoire de Génie Chimique, 118 Route de Narbonne, F-31062 Toulouse, France

^b CNRS, UMR 5503, F-31062 Toulouse, France

^c Université de Toulouse, INPT, UPS, Institut de Mécanique des Fluides, Avenue Camille Soula, F-31400 Toulouse, France

^d CNRS, UMR 5502, F-31400 Toulouse, France

ARTICLE INFO

Available online 26 October 2010

Keywords:

Fouling
Particle capture
Separation
Colloid
Microfluidic

ABSTRACT

In this paper, we examine the contributions of colloidal surface interaction in filtration processes. In a first part, we describe the way surface interactions affect the transport of colloidal particles or macromolecules towards a membrane, and its theoretical description. The concept of critical flux is introduced and linked to particle–membrane wall and particle–particle surface interactions. From this review, it seems important to consider how surface interactions occur at pore scale and control the development of fouling layers. In this context, we report in a second part experiments where the capture of micron-sized particles is observed in a poly-dimethylsiloxane (PDMS) microfluidic filtration device. Direct observations of the filtering part by video-microscopy allow to investigate the way the fouling of the microchannels by the particles is taking place. The experimental results underline the important role played by the particle–wall interactions on the way particles are captured during filtration. A small change in surface properties of the PDMS has important consequences in the way pore clogging occurs: in more hydrophobic conditions the particles first form arches at the microchannels entrance, then leading to the growth of a filtration cake, whereas in more hydrophilic conditions the particles are captured on the walls between the microchannels, then leading to the progressive formation of dendrites. To conclude, both experimental and theoretical approaches show the important role played by surface interactions in filtration processes. The complex interplay between multi-body surface interactions and hydrodynamics at nanometric scale leads to clogging phenomena observed experimentally in microfluidic systems that have not been predicted by numerical simulations. In the future, the two way coupling between simulation and experimental approaches at the pore scale have to progress in order to reach a full understanding of the contribution of colloid science in membrane processes.

© 2010 Elsevier B.V. All rights reserved.

Contents

1. Introduction	3
2. Surface interaction and the concept of critical flux: from the membrane scale to the pore scale	3
2.1. Critical flux and particles–membrane surface interactions	3
2.2. Critical flux and particle–particle surface interactions	4
2.3. Towards a pore scale approach	5
3. Experimental investigation of fouling mechanisms at pore scale	6
3.1. Materials and methods	7
3.1.1. PDMS micro-separator fabrication and characteristics	7
3.1.2. PDMS “conditioning” and surface properties	7
3.1.3. Latex suspensions	8
3.1.4. Filtration and visualization procedure	8
3.2. Results	8
3.2.1. Influence of particles stability on clogging	8
3.2.2. Influence of PDMS conditioning on the clogging	9
3.3. Discussion	10
4. Conclusions	10

* Corresponding author. Université de Toulouse, INPT, UPS, Laboratoire de Génie Chimique, 118 Route de Narbonne, F-31062 Toulouse, France.
E-mail address: bacchin@chimie.ups-tlse.fr (P. Bacchin).

Acknowledgements 10
 References 10

1. Introduction

The separation of micron-sized particles from a liquid using a filter is an important operation in numerous industrial processes (with environmental, chemical, pharmaceutical or biomedical applications). This separation can be achieved by different means such as deep-bed filtration, screen filtration and pressure-driven membrane filtration. These processes rely on the capture of particles within a porous medium (deep filtration) or at its surface (screen filtration). Particle capture is sometimes desired (deep-bed filtration), but in some cases it appears as a serious limitation of the process (fouling). The understanding of the way particles adhere to the surface and the reversibility of the capture process (by a phase change, a back-flush...) is a scientific challenge with important technical consequences. However, the mechanisms leading to particle capture (and/or detachment) in screen filtration and deep filtration are not yet fully well understood, mainly because of the complex interplay between hydrodynamic and physico-chemical interactions between the particles (generally dispersed colloids) and the collecting surface.

Our aim is to present some recent progresses in the understanding of the contribution of surface interactions on particle capture on a membrane. We report modelling and experiments shedding light on the effect of particle-particle and particle-wall surface interaction on fouling phenomena. In a first part, we show how the consideration of surface interactions at a macroscopic scale (at the scale of the porous surface) leads to define a critical flux resulting from a balance between drag forces and surface interaction forces. We further examine the consequences of surface interactions at a mesoscopic scale (at the pore scale). In a second part, the paper reports direct observations of particles capture and subsequent clogging of a PDMS microfluidic device, thereafter called “microfluidic-separator.” This device mimics a fraction of a filtration unit and allows to observe at the pore scale how particle capture is affected by surface interaction phenomena.

2. Surface interaction and the concept of critical flux: from the membrane scale to the pore scale

In past studies, it has been demonstrated that colloidal surface interactions are responsible of specific fouling behavior in membrane processes. Cohen et al. [1] were the first to postulate that surface interactions between colloidal particles could play a specific role. They noted that permeate flux obtained in reverse osmosis of ferric hydroxide dispersions was very high compared to the one expected from a balance between convection and classical dispersive forces

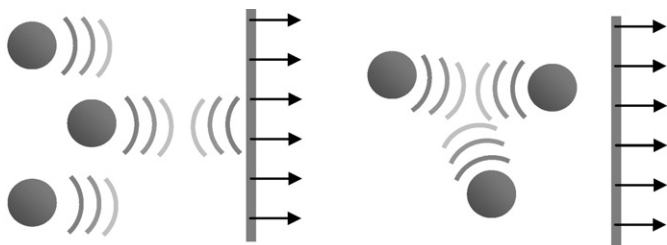


Fig. 1. Effect of surface interactions at a porous surface due to particle-wall interaction (a) and multibody particle-particle interactions (b).

(diffusion, lateral migration, shear induced diffusion) and named this the “colloid flux paradox.” In 1989, McDonogh et al. [2] developed this idea and reported experiments with silica particles where permeate flux was affected by changes of ionic strength. Since then, experimental results with various colloidal dispersions have shown that the particle colloidal stability is a key point to depict macroscopic variation in permeate flux. From a theoretical point of view, this effect has been examined by considering either particle-wall or particle-particle surface interactions (Fig. 1).

2.1. Critical flux and particles-membrane surface interactions

When considering the filtration of particles, a first approach is to consider a single colloid driven towards the porous surface by the convective flux, J . Mass transfer then results from a balance between a convective term (related to the drag force acting on the particle) and a diffusive term described by an interaction potential V , which can be modeled using, for instance, the DLVO theory [3].

Thus, as sketched in Fig. 2, the net flux of particles towards the membrane, N , is the combination of a convective flux and of fluxes which tend to remove particles away from the wall and which derive from “dispersive” effects [4]:

$$N = J\phi - D \frac{d\phi}{dz} - \frac{D}{kT} \phi \frac{dV}{dz} \tag{1}$$

The first term in the right hand side of this equation is the convective contribution to the flux, the second one, the contribution due to diffusion and the third one represents the term for migration of the solutes/particles due to surface interactions with the membrane. When surface interactions are repulsive, this latter term is opposed to the convective mass flux. When diffusion is neglectible, it is possible to determine conditions where the repulsive surface interactions balance convection thus leading to a nil mass flux. One can then define a critical permeation flux below which no particle deposition occurs as the drag force acting on the particle is not high enough to overcome the repulsion between the particle and the membrane. By integration of the continuity equation with Eq. (1), the critical flux has been

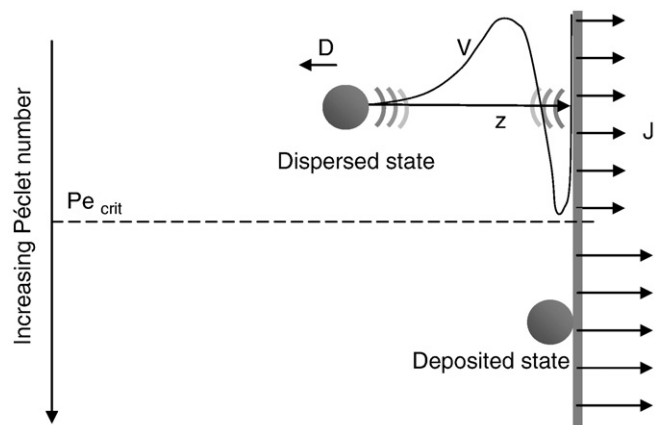


Fig. 2. Schematic representation of the links between particle-porous surface interaction and critical operating conditions for concentration processes.

linked [4] to the DLVO potential interaction barrier by the following relationship:

$$J_{crit} = \frac{D}{\delta} \ln\left(\frac{V_B}{\delta}\right) \text{ or } Pe_{crit} = \ln\left(\frac{V_B}{\delta}\right) \quad (2)$$

where δ is the mass boundary layer thickness. In the above relation, V_B quantifies the potential barrier of the particle-surface interactions and is related to the particle-surface interaction potential $V(z)$ by:

$$V_B = \int_0^\infty \left(e^{\frac{V(z)}{kT}} - 1 \right) dz \approx 2a(W-1) \quad (3)$$

Eq. (2) describes, from a theoretical point of view the effect of the colloids stability (effect of ionic strength, surface charge) on mass transfer towards the membrane and this can equivalently be expressed by using a critical Pe number. When considering similar surface properties for the particles and the membrane, the potential barrier, V_B , relative to particle-wall surface interaction can be linked to the classical stability ratio, denoted as W , defined for particle-particle interactions [3,5] between particles with a same radius, a .

Experimentally, the evidence of a critical flux below which no deposition occurs has been given since 1995 [6]. Sub-critical operations (i.e., conducted at a permeate flux below the critical flux) have shown the relevance of such a concept to various colloidal dispersions [7]. “Flux stepping” techniques have been developed to determine the critical flux and its dependence to the colloids stability [8–11]. Typically, using these techniques, the critical flux has been found to decrease when increasing the ionic strength with silica [2], clays [12] or latex particles [8,13], or when the pH approaches the isoelectric point for myoglobin [14], BSA [15], sodium caseinate [16] or silica [10]. However, the importance of the membrane surface charge on the critical flux seems to be less important. For instance, Huisman et al. [17] ran experiments on silica filtration using three membranes having the same cut-off but made with different membrane materials (titania, zirconia and α -alumina). No noticeable difference in the value of critical flux was observed even when the membrane zeta potential was changed from positive to negative values. Chan and Chen [15] emphasized this conclusion in a study focused on the precake formation, which showed evidence of the importance of membrane morphology for the limiting mechanisms only during sub-critical experiments (i.e., when the membrane is not covered by a layer of particles). A possible explanation for these discrepancies between theory and experiment is that the membrane could be rapidly covered with a layer of colloidal particles thus leading to single particle-particle like surface interactions rather than particle-membrane interactions.

2.2. Critical flux and particle-particle surface interactions

During a filtration process, the colloidal particles accumulate at the surface: a particle is not only interacting with the filter but also with neighbouring particles (Fig. 1b). Theoretically, it is possible to account for the contribution of multi-body particle-particle surface interaction in mass transport equations by using the notion of collective diffusion [5]. Collective diffusion accounts for the role of particle-particle interactions on the diffusion of particles in a concentration gradient. The collective diffusion coefficient is linked to the osmotic pressure via the generalized Stokes-Einstein relationship [18–21]:

$$D(\phi, V) = \frac{K(\phi)}{6\pi\mu a} V_p \frac{d\Pi}{d\phi} \quad (4)$$

where V_p is the particle volume and the osmotic pressure Π an equilibrium property of the colloidal dispersion which can be linked to multi-body particle interaction as follows [5,19]:

$$\Pi = nkT - \frac{2\pi}{3} n^2 \int_0^\infty r^3 g(r) \frac{dV}{dr} dr \quad (5)$$

where V denotes now the particle-particle interaction potential.

As expressed, the osmotic pressure depends on the number of particles per unit volume, n , their spatial distribution (through the radial distribution function, $g(r)$) and on the particle-particle interactions, V , determined with the DLVO theory for instance. The first term in the right-hand-side of Eq. (5) is the osmotic pressure expression in the dilute case. The second one gives the contribution of the particle-particle surface interactions to the osmotic pressure. As expected, this term is positive when these interactions are repulsive and negative when they are attractive, which is coherent with the fact that the osmotic pressure represents the propensity of the dispersion to resist against an increase in concentration. When particles are concentrated, the mean inter-particle distance is reduced. The short range van der Waals attractive interaction can then become larger than the long range repulsive interaction (as depicted through DLVO theory in terms of potential interaction energy to explain dispersion stability) resulting in a decrease of the positive slope $d\Pi/d\phi$. Theoretically, an instability (often called spinodal decomposition [5]) is reached when the derivative of the osmotic pressure with the volume fraction is equal to zero. Such a transition between a dispersed state and a solid state [Fig. 3] occurs for a critical volume fraction, ϕ_{crit} , associated to a critical osmotic pressure, Π_{crit} [22]. Computing Π is rather difficult and inaccurate for complex dispersions mainly because of the assumptions made when using DLVO theory [3]. However, one main advantage of using the osmotic pressure is that it is experimentally accessible by different techniques (chemical compression [8,23], membrane osmometry, ...). Furthermore, during this kind of measurement, it is possible to detect the phase transition (by associating analysis of packing reversibility [8,24] or rheology [23]) and then to build phase diagrams [25,26]. Osmotic pressure is experimentally sensitive to the parameters of colloidal interaction [8,23,26,27] and is a convenient property to account for the effect of multi-body colloidal surface interactions. In term of diffusivity (Eq. (4)), a large sensitivity of Π to ϕ leads to high diffusion coefficients (repulsion act as springs which are compressed because of the concentration and can be “released” in a concentration gradient [28]). For high volume fractions (i.e., small separation distance) attraction becomes important, and the diffusion coefficient is reduced.

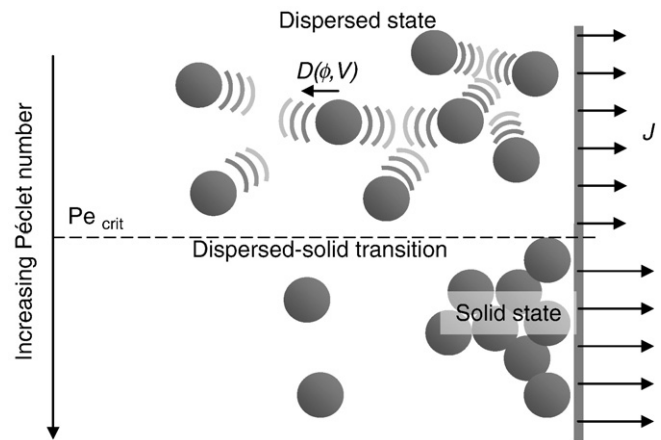


Fig. 3. Schematic representation of the links between colloidal surface interaction, phase transition, osmotic pressure and critical operating conditions for concentration processes.

Diffusion tends to zero when spinodal decomposition occurs (this nil value is synonymous of irreversibility: the mass cannot return naturally to the bulk by diffusion).

When multi-body surface interactions occurs, the net flux of particles towards the membrane is given by:

$$N = J\phi - D(\phi, V) \frac{d\phi}{dz} = J\phi - \frac{K(\phi)}{6\pi\mu a} V_p \frac{d\Pi}{dz} \quad (6)$$

where the second term accounts for the multi-body surface interactions and can be written either using a modified diffusion coefficient, function of Φ and V (“interaction induced diffusion” [20,21]) or equivalently using the gradient of osmotic pressure [29].

Integration along z of the continuity equation with the above form of the mass flux equation (Eq. (6)) allows to determine the concentration profile in stationary state. It leads to the definition of filtration conditions for which the critical volume fraction is reached at the membrane surface leading to a spinodal decomposition. This occurs when the concentration is sufficiently high (or interparticle distance low enough) so that attraction between particles overcome the dispersive forces, thus leading to a transition from a dispersed to a solid state. This liquid/solid phase transition can be linked to the formation at the membrane of a deposit or a precipitate (for lyophobic colloid) or a gel (for lyophilic colloid).

Previous experimental works have shown that this transition occurs differently according to the process conditions (wall shear stress [30,31] and permeate flux [12]). As before, from a theoretical point of view, one can introduce a critical Péclet number above which a solid phase appears at the membrane surface; i.e., when the osmotic pressure at the membrane reaches its critical value as shown in Fig. 3. The Péclet number deduced from the integration of Eq. (6) allow to relate the critical operating conditions of the filtration processes (permeate flux, cross-flow velocity ...) to the properties of the material being concentrated (dispersion size, colloidal surface interaction) [29,32,33].

In cross-flow filtration, the formation of a solid phase at the membrane surface is related both to the permeate flux and to the cross-flow velocity (through the boundary layer thickness, δ) so that the relevant critical Péclet number can be defined as:

$$Pe_{cf\,crit} = \frac{J\delta}{D_0} = \frac{V_p}{kT} \int_{\Pi_b}^{\Pi_{crit}} \frac{K(\phi)}{\phi} d\Pi \quad (7)$$

The formation of a solid phase is favored by a high permeate flux and a thick boundary layer. It is possible to define the conditions in permeate flux, J and cross-flow velocity for which a solid phase can form on the membrane (conditions of high flux and low cross-flow velocity) or in contrast the conditions for which no solid phase forms (Fig. 4A).

In dead-end filtration, the critical Pe number reflects the combined effect of the permeate flux and of the accumulated mass of particles, V_a (proportional to the filtered volume, V_f) as follows [33]:

$$Pe_{de\,crit} = \frac{JV_a}{D_0} = \frac{V_p}{kT} \int_{\Pi_b}^{\Pi_{crit}} K(\phi) d\Pi \quad (8)$$

There are combinations of parameters “permeate flux/filtered volume” for which the solid phase is formed (or not formed) at the membrane surface. No solid phase is formed for conditions of low permeate flux and low filtered volume (Fig. 4B). These conditions are less restrictive for more stable dispersions.

Knowing these critical conditions allows to avoid the formation of a solid phase during filtration, in the so-called sub-critical operating conditions [34]. It has to be noted that the zone of no solid phase formation is reduced when the stability of colloidal dispersion is reduced (transition lines in Fig. 4 shift). The absence of a solid phase (by definition an irreversible phase) avoids subsequent deposition and the corresponding fouling removal steps. In cross-flow filtration, low permeate flux and high cross-flow velocity lead to a steady state flux without formation of solids at the membrane. In dead-end filtration, particles gradually build-up over time and require periodic back wash or surface flushing. Studies have shown [35,36] that rinsing before reaching the critical filtered volume (i.e., before reaching a critical filtration time) allows to perform successive filtration and rinse steps without solid phase formation at the membrane. The approach presented in this section can be extended to other concentration processes where the concentration can lead to colloidal phase transition (sedimentation, centrifugation, film drying ...) [29].

2.3. Towards a pore scale approach

This brief review shows how surface interactions play an important role in the different ways colloidal particles can behave at a filter surface. The critical flux concept has shown its relevance to understand how the dispersion stability combines to the filtration conditions and leads to very different fouling scenarios. However, a sharp transition between a dispersed and a solid phase is not often observed in practice and discrepancies between the models and experiments still exist [8,37] even with well-characterized suspensions and membranes.

One possible cause for these discrepancies is the fact that any membrane cannot be represented as a continuous porous surface with homogeneous properties. The topography of the membrane (porosity, cut-off, pore shape,...) has been shown to influence the experimental critical flux is concerned. Wu et al. [11] observed a decrease in the critical flux when the PES membrane cut-off is increased (Table 6 in [11]). As proposed by these authors, the change in critical flux could result from the difference in surface properties (such as charge) but

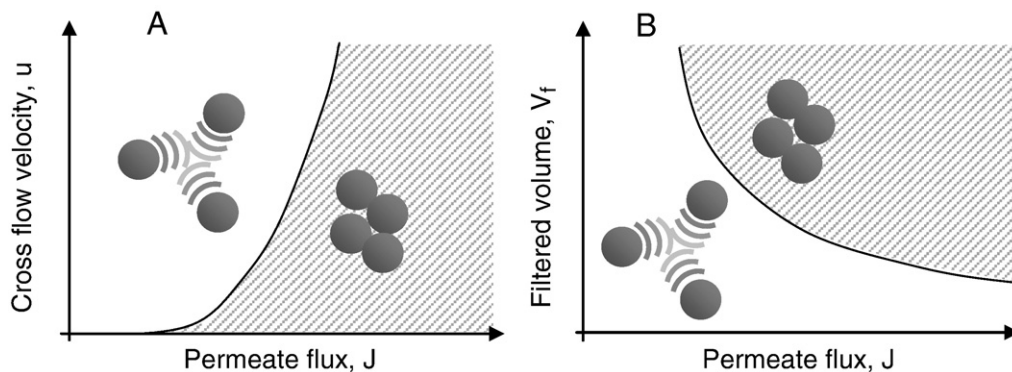


Fig. 4. Operation conditions leading to the presence (hatched zone) or to the absence of solid phase at the membrane for cross-flow (A) and dead-end (B) filtration.

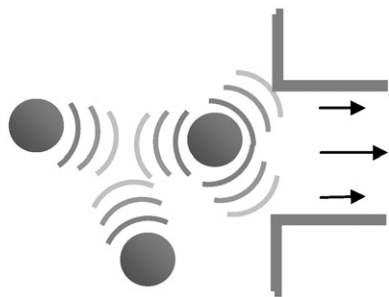


Fig. 5. Particles accumulation at a pore scale: effect of particle–wall interaction and multibody particle–particle interactions.

also from a change in local porosity and hence in local permeate velocity. The latter would locally modify the balance between drag force and surface interactions. Bromley et al. [38] showed a five-fold higher critical flux with slotted pores that with circular pores. These results clearly indicate the impact of the local structure at the membrane surface on the critical flux. Furthermore, other experiments with microsieves reported by Kuiper et al. [39] with circular pores but various porosities have shown that the latter plays an important role in the development of the cake layer at the membrane surface. For high porosity, i.e., pores very close to each other, steric hindrance can occur between particles and prevent their deposition over the whole membrane surface. Then, even if the critical flux is exceeded, the deposit cannot develop on the whole surface.

Even if the membrane were perfectly homogeneous, an uneven distribution of the permeate flux (locally, on the membrane) can nonetheless be observed in actual process applications. Ognier et al. [40] suggested that local changes in water flux are induced by the blockage of some pores. When operating at constant flux, this blockage in turn induces an increase in flux through the pores that remain open. Therefore, because of the resulting permeate flux heterogeneities, the critical conditions for a deposit to form near the membrane surface can be met locally, even if the mean conditions are sub-critical when considering the membrane as a homogeneous porous surface.

The results mentioned above highlight the need for studies performed at pore scale, in order to progress towards a better understanding and prediction of membranes fouling mechanisms. At that point, it is worth mentioning that even if the so-called filtration laws are based on fouling models involving a description at the pore scale, such as complete or intermediate pore blocking, pore section narrowing [41], they are typically used at membrane scale, to describe for instance the decline in permeate flux as fouling goes on. Thus, they are not able to properly model situations where membrane heterogeneity is important [42].

At pore scale, the exact description of the surface interactions between an isolated particle and the membrane is difficult when the particles and pore sizes are of the same order of magnitude (Fig. 5). In this case, one cannot simply use the results established by considering the membrane as a flat homogeneous plane (such as the one giving the DLVO potential for a sphere-infinite plane geometry, for instance) and a more realistic approach has to be developed. This significantly complicates any calculation of particle–membrane interactions [43–46]. Also, the description of the particle convective motion towards the membrane is also made much more complex when working at pore scale, as the hydrodynamic interactions between the particle and the membrane have to be accounted for. This can be done via enhanced drag coefficients, the determination of which requires complex numerical computations, even in the apparently simple case of a single particle approaching a cylindrical pore opening in a plane (see, for instance [47] and references therein). Furthermore, when the particle is getting close to the membrane surface, lubrication forces have to be taken into account. This overall picture is of course even

more complex when several particles approach simultaneously the pore as would be the case in a dense dispersion or when accumulation of particles at the membrane surface is occurring.

A limited number of studies have coped with the above mentioned difficulties, associated with a description of the fouling at pore scale. In 1999, Bowen et al. [44] computed the electrostatic interaction between a single charged particle near a pore, modeled as a cylindrical opening in a flat charged plane, for various particle positions. They found some equilibrium positions for the particle, located above the pore when the drag force exerted by the particle (corrected for pore-particle hydrodynamic interactions) is balanced by the repulsive electrostatic interaction. If the fluid velocity exceeds a given critical value, the drag force can overcome the repulsive force and the particle can flow through the pore. This is, at pore scale, a picture similar to the one of the critical flux concept, developed at the membrane scale and presented in the previous sections. Similar situations were experimentally evidenced by Ramachandran and Fogler [48,49], using direct visualizations of track-etched membranes, at pore scale, after filtration experiments performed with well latex dispersions of well controlled particle sizes.

Particle trajectories, accounting for the hydrodynamics and surface interactions at pore scale can also be numerically computed [50–54]. Several papers [50–52] reported critical velocities similar to the ones presented above. As far as experimental studies are concerned, one difficulty is to be able to extract meaningful data from experiments performed with real, heterogeneous (in term of pore size and spatial repartition) membranes. An alternative, still rarely found in the literature is to use model membranes, with a well controlled pore geometry [55–57].

Thus the development of novel, non-invasive, *in-situ* experimental methods is a key point for improving our understanding of particles capture by a porous medium [58].

3. Experimental investigation of fouling mechanisms at pore scale

Several recent experimental studies based on the use of microfluidic devices have been performed to visualize pore clogging and/or the formation of the first layers of particles. Some of these studies use microsieve membranes, i.e., very thin silicon screens with patterned holes. The fabrication of such membranes has been made possible by recent progresses in micro-engineered membrane technology [59]. Brans et al. [60] observed particle capture on a microsieve membrane [61], by microscopy or confocal scanning laser microscopy. Direct observations of the membrane top surface allow to make a distinction between the behavior of small particles (1 μm), that deposit at the circular pore edges and inside the pores, and of larger ones (10 μm), that deposit exactly onto the pores. By a statistical analysis of the deposition locations near the circular pores of a microsieve, Lin et al. [56] showed that particles smaller than the pore are preferentially captured at two positions: either close to the pore edge and or located one particle radius away from the pore center, compared to the first one.

Microfluidics systems made of PDMS have also been used to develop micro-separators, typically consisting in an array of parallel, narrow channels which act as a filter. These devices allow to have a “side view” of the pores, which is complementary to the top view obtained in the aforementioned studies using microsieves. They have been used to filtrate latex particles in dead-end mode [57] or red blood cells in a cross-flow mode [62,63]. In dead-end mode, Wyss et al. [57] measured the blockage time of the microfluidic channels in order to determine the physical processes governing single-pore clogging. Groisman et al. [62] and Chen et al. [63] designed micro-separators working in cross-flow mode for the separation of plasma from whole human blood by size exclusion, a potential application being the development of microanalysis system for point-of-care diagnostics. The performance of such devices was seen to be substantially improved with pulsatile pressure (back-pulsing) [62]

and by increasing cross-flow velocity [63], as in macroscale cross-flow filters.

3.1. Materials and methods

The present experiments have been performed with PDMS devices similar to those presented in [57]. They operated in dead-end mode, at a constant filtration flow rate. Direct observation, by digital video microscopy, of particles accumulation at the entrance or inside the micro-channels was made possible by the use of PDMS, which is transparent. Particle capture depended on the microchannels geometry (width and length) and on the hydrodynamics and physico-chemical conditions.

3.1.1. PDMS micro-separator fabrication and characteristics

The PDMS micro-separators used in the present study were made by the usual soft lithography technique [64]. A sketch of the PDMS micro-separators is shown in Fig. 6. The depth of all the channels of the network was 50 μm . The filtering part of the device consisted in a parallel arrangement of 27 micro-channels. Each microchannel had a set of constrictions along its length such that the smallest width was 20 μm . The distance between the centers of two successive micro-channels was 68 μm . The divergent shape of the main single channel, up to the microchannels, was designed to ensure a homogeneous flow of the suspension, over the width of the filtering part.

3.1.2. PDMS “conditioning” and surface properties

The PDMS micro-separator was first cleaned with a Hellmanex solution diluted at 1/1000. Before filtration, the micro-separator was rinsed with a 10^{-1} M KCl solution (KCl conditioning) or with ultrapure water (water conditioning). It has been shown that the rinse with these two solutions change surface properties. The wettability of the PDMS has been estimated with the sessile drop and the captive bubble techniques with five different liquids (water, diiodomethane, glycerol, formamide, ethylene glycol) on a Digidrop apparatus (GBX, Romans, France). The use of the Owens-wendt relationship [65] allows to estimate the polar, γ_S^p , and non polar (or dispersive), γ_S^d contributions to the total surface energy (see Table 1). With the sessile drop technique, surface energies are close to the one referenced [65] for PDMS materials ($\gamma_S^d = 19 \text{ mJ/m}^2$ et $\gamma_S^p = 0,8 \text{ mJ/m}^2$). The captive bubble technique give higher values of surface energies ; this difference being normal for materials having positive wetting hysteresis [65]. When comparing PDMS surfaces after KCl or water conditioning, these two techniques show that the surface energies are slightly higher for KCl conditioning, resulting in a slightly more hydrophilic surface.

Table 1
Wettability of PDMS.

	Surface energy of PDMS surface in mJ/m^2	
	Water conditioning	KCl conditioning
<i>Immerged bubble technique</i>		
γS^D	25,7	24,8
γS^P	28,3	33,8
γS	54	58,6
<i>Deposited drop technique</i>		
γS^D	13,6	19,7
γS^P	1	0,16
γS	14,6	19,86

Attenuated total reflectance on Fourier transform infrared (ATR-FTIR) analysis has also been performed on PDMS surface with a Nicolet Nexus spectrometer. Fig. 7 shows the ATR-FTIR spectra of PDMS after the two conditioning steps. The ATR-FTIR data shows the expected peaks of PDMS at 1256 cm^{-1} (stretching of the aliphatic Si-CH₃ group), 1015 cm^{-1} (Si-O-Si asymmetric deform) and 790 cm^{-1} (Si-(CH₃)₂) for both samples [66]. An important difference between samples is found at higher wave number. The sample conditioned with KCl shows a higher peak corresponding to the broad adsorption of OH bond of water molecules (3410 cm^{-1}) and of OH group of silanol (3450 cm^{-1}). The higher wettability of PDMS after the KCl conditioning measurement might be attributed to these groups.

Changes in PDMS surface properties by grafting or adsorption of ligands are frequently implemented and shown to have quite strong effects on the hydrophilic/hydrophobic character of micro-systems. However, to our knowledge, there is no report of the changes in the physico-chemical properties of PDMS caused by a contact between PDMS and water containing a salt which could help to interpret the present results. However, it could be supposed (at the light of the role played by salt solution in the elution of chromatography support) that the conditioning of the PDMS micro-separator with a saline solution could induce an elution of macromolecules which would be present in the bulk of the PDMS material because of the fabrication process (uncross-linked of PDMS oligomers) or because of an unwanted contamination (from the Hellmanex solution or other molecules present in water). The uncross-linked PDMS oligomers have been shown [67] to be responsible of the long term change (time-scale of days) of a plasma-activated hydrophilic PDMS surface to a hydrophobic state after surface rearrangements at the molecular scale, that bring new hydrophobic groups to the PDMS surface. The extraction of these PDMS oligomers from the bulk polymer with solvents leads to

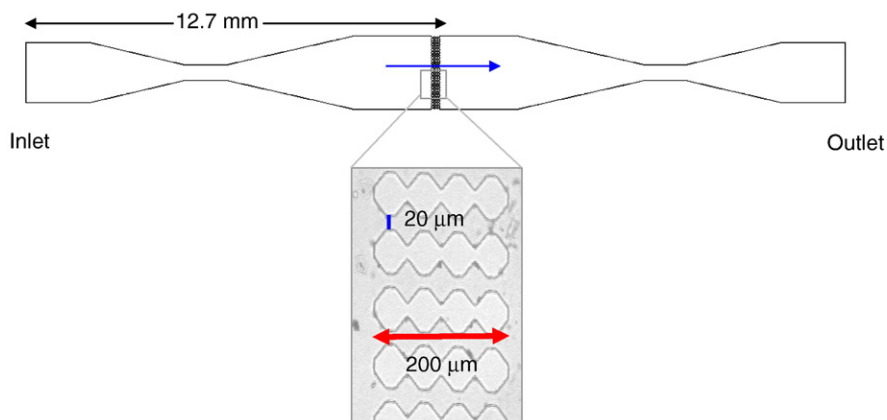


Fig. 6. Sketch of the PDMS micro-separators (top) with an image centered on some of the microchannels (bottom). The whole filtering part of the device consisted of a parallel arrangement of 27 microchannels.

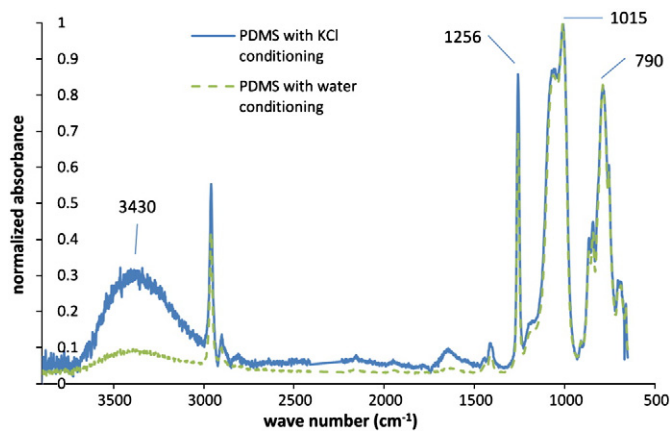


Fig. 7. ATR-FTIR spectra for PDMS after (a) KCl conditioning and (b) water conditioning.

have hydrophilic surfaces that slowly regenerate into hydrophobic surfaces [67]. Klammer et al. [68] showed that PDMS requires a pre-conditioning in alkaline solution for 5–6 days before starting biocatalytic reactions. We believe that the conditioning of a PDMS surface with a saline solution could lead to similar surface modifications.

3.1.3. Latex suspensions

The suspensions used in the present study consisted in monomodal polystyrene microspheres (latex) dispersed in water. Surfactant-free concentrated particles suspensions were purchased from Invitrogen. The latex particles were $4.9 \pm 0.21 \mu\text{m}$ in diameter and negatively charged with functional sulfate groups on the surface: the zeta potential, measured with a Malvern Zetasizer, was $-57 \pm 5 \text{ mV}$ at pH 7.

The latex suspensions used in the filtration experiments were obtained by diluting stock suspension in KCl solution until a volume fraction of 10^{-3} was reached. The KCl concentration was varied in the range 10^{-5} to 10^{-1} M which allowed to modify the suspension stability by changing the magnitude of the repulsive electrostatic interaction between particles. These concentrations in salt were inferior to the critical concentration for coagulation which was observed by sedimentation tests to be above $2 \cdot 10^{-1} \text{ M}$. Prior to experiments, the latex suspensions were observed under microscope to check for the absence of aggregates. Note that such salinity changes also possibly modified the interaction between the particles and the micro-separator PDMS surface.

3.1.4. Filtration and visualization procedure

In dead-end mode, a constant filtration flow rate ($q = 2 \text{ ml/h}$) was imposed through the micro-separators by a syringe pump (Sky

Electronic PS 2000). The pressure at the micro-separator inlet (also representative of the pressure drop through the micro-separator) was measured with a pressure gauge (PR41, Keller). The micro-separator was placed on the platform of an Axiolab (Zeiss) microscope, (Fig. 8), and images were captured using a high sensitivity camera (Pixelfly QE, PCO). The exposure time for the camera was 6 ms. The dynamics of the micro-channels clogging could then be studied using the recorded images at the micro channel scale. The location of the captured particles (for the very first layers of particles) and, later on, the cake were easily distinguished on the images.

3.2. Results

The results presented in this paper correspond to a technologically important regime in solid/liquid filtration or microfiltration: filtration of a dilute suspension (volume fraction = 0.001) at a high imposed flow rate ($q = 2 \text{ ml/h}$, i.e., $16.2 \text{ m}^3/\text{h}$ per square meter of “filter”). For this flow rate, the Reynolds number in the large upstream channel was $Re = U d_H / \nu_f = 0.44$, where d_H is the hydraulic diameter, U the typical velocity ($U = 4.5 \text{ mm/s}$) and ν_f the fluid kinematic viscosity. The Reynolds number for the flow in a microchannel was 0.58 (typical velocity: 20.5 mm/s). Particle sedimentation can be neglected as the particle settling time (the settling velocity is $O(1) \mu\text{m/s}$) over the height of the microchannel ($50 \mu\text{m}$) was much larger than the particle residence time in a microchannel (10 ms).

Inertial effects, which would make the particles deviate from the fluid streamlines when the latter bend close to a microchannel entrance, can be quantified by a Stokes number which is the ratio of the particle viscous relaxation time, $\tau_v = 2a^2\rho_p/9\mu_f$, to a typical time scale for the flow through the orifice, $\tau_f = d_p/U$, where d_p is a characteristic microchannel dimension. Using the estimate obtained above for the fluid velocity, ($U = 20.5 \text{ mm/s}$), and taking $d_p = 20 \mu\text{m}$, the Stokes numbers, are in the range $O(10^{-5} - 10^{-3})$ so that inertial effects can be neglected.

The effect of Brownian diffusion can be evaluated by the ratio of a typical timescale for the Brownian diffusion of the particles towards the pore edge, τ_d , to the time scale for the flow through the orifice, τ_f . Here, $\tau_d = d_p^2/D_B$, where D_B is the Brownian diffusivity coefficient given by the Stokes–Einstein formula $D_B = k_B T / 6\pi\eta a$ (where k_B is the Boltzmann constant). The Péclet number thus obtained, $Pe = \tau_d/\tau_f$, are very large, $O(10^5 - 10^6)$, so that Brownian motion effects can be neglected as well.

3.2.1. Influence of particles stability on clogging

As already mentioned, filtration experiments have been performed for various KCl concentrations. The salt concentration had an important effect on the capture rate. No particle capture was observed when the KCl concentration was below 10^{-2} M . Particle capture

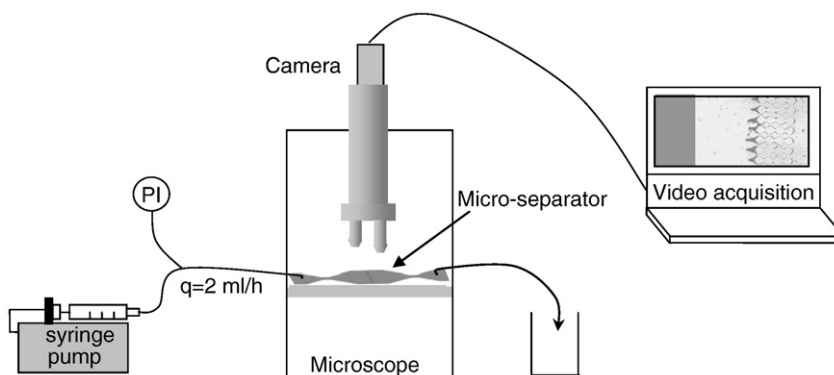


Fig. 8. Sketch of the experimental set-up.

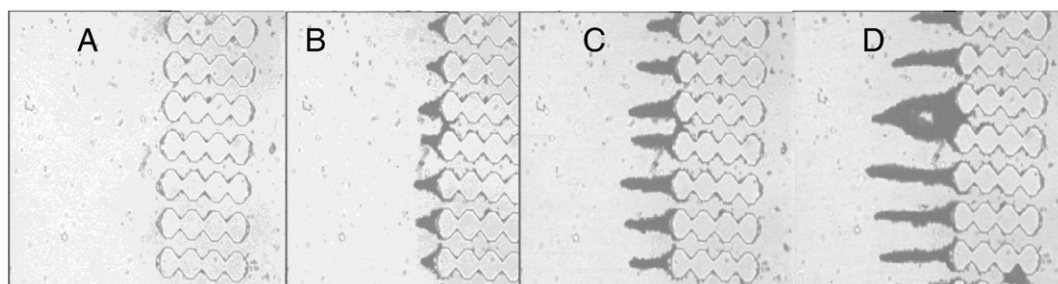


Fig. 9. Observation of particle capture after a conditioning of the micro-separator with a KCl solution, leading to the formation of dendrites. Image A was taken at $t_0 + 1$ min (at t_0 , the suspension starts flowing into the microchannels), image B at $t_0 + 20$ min, image C at $t_0 + 45$ min and image D at $t_0 + 90$ min.

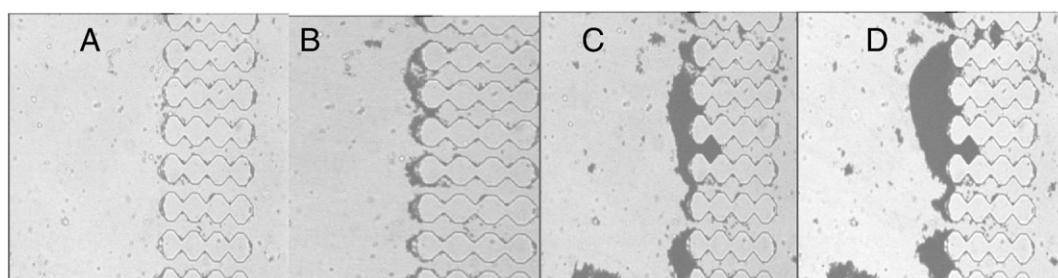


Fig. 10. Observation of particle capture after a conditioning of the micro-separator with ultrapure water, leading to the progressive obstruction of the microchannels, and then formation of a filtration cake. Image A at $t_0 + 1$ min, image B at $t_0 + 20$ min, image C at $t_0 + 45$ min and image D at $t_0 + 90$ min.

became observable at 10^{-2} M (few particles were captured on the micro-separator walls) and was relatively important at 10^{-1} M (channel clogging was significant). These results show that the suspension stability had an important effect on particle capture: when the salt concentration increased, the repulsive electrostatic interaction between the particles was reduced, which promoted particle–particle adhesion. Note that it also possibly changed the interaction between the particles and the micro-channels PDMS walls. As already mentioned in studies on particle deposition [69] these interaction have an important effect on particle capture. Experimental results presented in the next subsection were obtained with a KCl concentration of 10^{-1} M, in order to reach a particle capture rates during the experiments that allows to observe the clogging phenomena. However, it has to be noted that the capture efficiency stays very

low (less than 1%) as long as a dense deposit is not formed at the PDMS microfluidic separator filtering part surface.

3.2.2. Influence of PDMS conditioning on the clogging

The micro-separator clogging was found to be highly sensitive to the conditioning step of the micro-separator (see Section 3.1.2). Figs. 9 and 10 show the gradual development of the micro-separator clogging, for the 10^{-1} M KCl conditioning and for the ultrapure water conditioning, respectively. KCl conditioning (Fig. 9) led to the formation of dendrites. After 90 min of filtration, the length of these dendrites could reach more than 200 μm , i.e., 40 particle diameters. Ultrapure water (Fig. 10), led to a gradual obstruction of the microchannels, provoking the progressive and continuous growth of

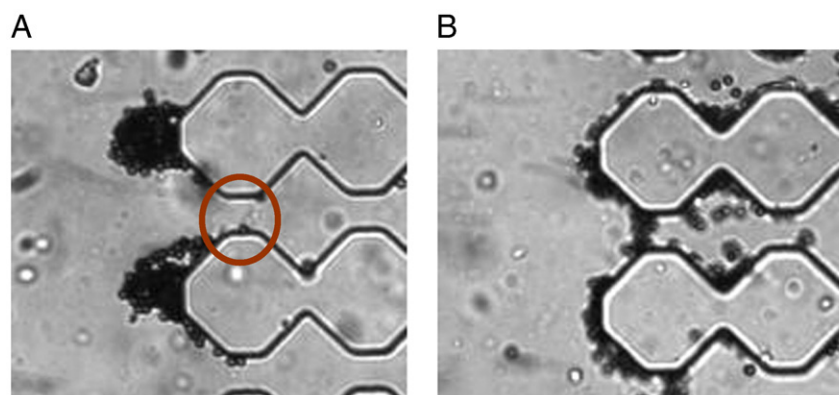


Fig. 11. Observation of the first stages of the particle capture. (A) After a PDMS conditioning with a KCl solution (image taken 1 min after the beginning of the filtration experiment). (B) After a PDMS conditioning with ultrapure water (image taken 30 s after the beginning of the filtration experiment). The formation of arches at the entrance of microchannels is clearly seen in image (B), whereas such a capture is not seen in (A).

a filtration cake. The cake formation was not homogeneous on the micro-separator: some channels could stay open whereas others were already completely clogged.

From a detailed visual inspection of the recorded images, we conclude that the clogging of the microchannels, as observed in Fig. 10, was induced by arches formed at the microchannels entrance (Fig. 11B). These arches led to pore blocking, which in turn led to the formation of a compact filtration cake. On the contrary, when dendrites were formed (Fig. 9), there was no capture of particles at the microchannel entrance (i.e., in the region highlighted by a circle in Fig. 11A). Then, arch formation and the subsequent clogging did not happen. As the present filtration experiments were performed at a constant flow rate, clogging of the micro-separator resulted in an increase in the pressure drop less important for KCl conditioning.

3.3. Discussion

Experiments show the effect of surface interactions on the way particles are captured at a pore entrance. Surprisingly, a slight change in surface interaction conditions leads to very different clogging patterns. For a more hydrophilic PDMS surface materials (after KCl conditioning as shown in Section 3.1.2) the collision efficiency on the PDMS wall at the microchannels entrance is very low. Very few particles are captured in the zone encircled in Fig. 11a corresponding to the bottleneck of the microchannels and dendrites are then preferentially formed. On the contrary, in more hydrophobic conditions (water conditioning), the formation of arches could be promoted by efficient lateral collisions between particles and the wall, on the bottleneck zone. Concerning this latter mechanism, it has been shown [70], by observation of particle flow in microtubes (100 μm in diameter), that their blockage by arches formation is more likely to occur when the particle to tube diameter ratios is approximately 0.3–0.4, even for low volume fraction (0.005 in [70]). The experimental conditions of the present experiments, with a particle to microchannel width ratio of 0.25 and for volume fraction of 0.001, were therefore close to the ones for which particle arching is likely to occur, according to [70]. These arches led to a progressive clogging of microchannels and then to a quick growth of the deposit on the surface. Dendrites formation should then be favored when there are no efficient lateral collisions between the flowing particles and the bottleneck wall, so that particles arching is not likely to occur.

Even if these results cannot prove a direct link between hydrophobic/hydrophilic character of the material and the fouling behavior, they illustrate how surface interaction can impact fouling. To have a better understanding, it is now necessary to develop simulation that allow checking how a change in particle–wall surface interaction lead to different clogging pattern and thus fouling behavior. To do that, it is necessary to develop multi-particle simulation at the pore scale accounting for the interplay between hydrodynamics and surface interaction phenomena.

4. Conclusions

Surface interactions play undeniably an important role in the way fouling layers form during membrane filtration. Taking into account these surface interactions has been a major breakthrough in the understanding of fouling but also on its controls using the critical flux concept. However, the predictability with actual theories and simulations is still unsatisfactory. This lack in predictability is a problem for practitioners and technologists. As discussed on this paper, a possible explanation for discrepancies between theory/simulations and experiments is that the theoretical modelling and numerical simulations often neglect multi-body interactions by considering only surface interactions between pairs of particles (thus neglecting multi-body interaction) and also often represent the membrane as an homogeneous material (thus neglecting the phenomena occurring at

the pore scale). In this context, microfluidic separators in PDMS has been developed to allow in-situ clogging observation at the pore scale. These experiments are performed with a well-defined geometry and controlled hydrodynamic and physico-chemical conditions. Two different modes of particles capture have been evidenced in our filtration experiments depending on the hydrophilic properties of the PDMS device. The clogging mode occurring in more hydrophobic conditions has important consequences on the efficiency of the separation: particles arches form at the microchannel entrance, thus leading to a fast and complete fouling of the microchannels. On the contrary, the dendrites that appear when the PDMS is more hydrophilic offer a much lower resistance to the flow. Also, this clogging mode is much less efficient in term of particle capture as particles can still flow through the filtering part of the micro-separator, even when long dendrites have developed. The formation of dendrites seems to be favored when there are no efficient lateral collisions between the flowing particles and the wall at the microchannel entrance. The present study illustrates how the balance between particle transport and particle–wall interactions (which are sensitive to the PDMS conditioning) controls the mechanisms of particle capture. Progress in understanding the clogging mechanism in such model filters is an essential first step in controlling fouling of real porous materials.

Acknowledgements

The authors thank Alexandre Chamoux for its contribution to the experimental work on the measurement of PDMS wettability. The authors acknowledge the “Federation FERMAT” (FR CNRS 3089) for partly funding this research work and David Bourrier from the “plate-forme technologique du LAAS (UPR CNRS 8001)” for technical support in the fabrication of the micro-separators.

References

- [1] Cohen RD, Probstein RF. *J Colloid Interface Sci* 1986;194:207.
- [2] Mcdonogh RM, Fane AG, Fell CJD. *J Membr Sci* 1989;69:85.
- [3] Verwey EJW, Overbeek JThG. Theory of the stability of lyophobic colloids: the interaction of sol particles having an electric double layer. Elsevier; 1948.
- [4] Bacchin P, Aïmar P, Sanchez V. *AIChE J* 1995;41:368–77.
- [5] Russel WB, Saville DA, Schowalter WR. *Colloidal Dispersions*. Cambridge University Press; 1989.
- [6] Field RW, Wu D, Howell JA, Gupta BB. *J Membr Sci* 1995;259:272.
- [7] Bacchin P, Aïmar P, Field R. *J Membr Sci* 2006;42:69.
- [8] Espinasse B, Bacchin P, Aïmar P. *J Colloid Interface Sci* 2008;483:490.
- [9] Espinasse B, Bacchin P, Aïmar P. *Desalination* 2002;91:96.
- [10] Chen V, Fane AG, Madaeni S, Wenten IG. *J Membr Sci* 1997;109:122.
- [11] Wu DX, Howell JA, Field RW. *J Membr Sci* 1999;152:89–98.
- [12] Bacchin P, Aïmar P, Sanchez V. *J Membr Sci* 1996;115:49–63.
- [13] Kwon DY, Vigneswaran S, Fane AG, Ben aim R. *Sep Purif Technol* 2000;19:169–81.
- [14] Metsamuuronen S, Howell J, Nystrom M. *J Membr Sci* 2002;196:13–25.
- [15] Chan R, Chen V. *J Membr Sci* 2001;185:177–92.
- [16] Youravong W, Grandison AS, Lewis MJ. *J Dairy Res* 2002;69:443–55.
- [17] Huisman IH, Vellenga E, Tragardh G, Tragardh C. *J Membr Sci* 1999;156:153–8.
- [18] Einstein A. *Investigation on the Theory of the Brownian Movement*. Dover Publications; 1956.
- [19] Van den Broeck C, Lostak F, Lekkerkerker HNW. *J Chem Phys* 1980;74.
- [20] Petsev DN, Denkov ND. *J Colloid Interface Sci* 1992;149:329–44.
- [21] Bowen WR, Liang YC, Williams PM. *Chem Eng Sci* 2000;55:2359–77.
- [22] Jönsson AS, Jönsson B. *J Colloid Interface Sci* 1996;180:504–18.
- [23] Bonnet-Gonnet C, Belloni L, Cabane B. *Langmuir* 1994;10:4012–21.
- [24] Martin C, Pignon F, Magnin A, Meireles M, Lelièvre V, Lindner P, et al. *Langmuir* 2006;22:4065–75.
- [25] Mourchid A, Lecolier E, Van Damme H, Levitz P. *Langmuir* 1998;14:4718–23.
- [26] Michot LJ, Bihannic I, Porsch K, Maddi S, Baravian C, Mougél J, et al. *Langmuir* 2004;20:10829–37.
- [27] Tsao YH, Evans DF, Rand RP, Pargesian VA. *Langmuir* 1993;9:233–41.
- [28] Petsev DN, Starov VM, Ivanov IB. *Colloids Surf A* 1993;81:65–81.
- [29] Bacchin P, Aïmar P. Concentrated phases of colloids or nanoparticles: Solid pressure and dynamics of concentration processes, chapter. In: Starov V, editor. *Nano: science:colloidal background*. CRC Press; 2010.
- [30] Madaeni SS, Fane AG, Wiley DE. *J Chem Technol Biotechnol* 1999;74:539–43.
- [31] Gesan-Guizou G, Boyaval E, Daufin G. *J Membr Sci* 1999;158:211–22.
- [32] Bacchin P. *J Membr Sci* 2004;228:237–41.
- [33] Bacchin P, Aïmar P. *Desalination* 2005;175:21–7.
- [34] Howell JA. *J Membr Sci* 1995;107:165–71.

- [35] Bessiere Y, Nouhad A, Bacchin P. *J Membr Sci* 2005;264:37–47.
- [36] Defrance L, Jaffrin MY. *J Membr Sci* 1999;157:73–84.
- [37] Bacchin P, Espinasse B, Bessiere Y, Fletcher DF, Aïmar P. *Desalination* 2006;192:74–81.
- [38] Bromley AJ, Holdich RG, Cumming IW. *J Membr Sci* 2002;196:27–37.
- [39] Kuiper S, van Rijn CJM, Nijdam W, Krijnen GJM, Elwenspoek MC. *J Membr Sci* 2000;180:15–28.
- [40] Ognier S, Wisniewski C, Grasmick A. *Desalination* 2002;146:141–7.
- [41] Hermia J. *Chem Eng Res Des* 1982;60:183–7.
- [42] Grenier A, Meireles M, Aïmar P, Carvin P. *Chem Eng Res Des* 2008;86:1281–93.
- [43] Bhattacharjee S, Sharma A. *J Colloid Interface Sci* 1995;171.
- [44] Bowen WR, Filippov AN, Sharif AO, Starov VM. *Adv Colloid Interface Sci* 1999;81.
- [45] Bowen WR, Sharif AO. *Colloids Surf A* 2002;201.
- [46] Bowen WR, Sharif AO. *Colloids Surf A* 2002;201:207–17.
- [47] Kao JN, Wang Y, Pfeffer R, Weinbaum S. *J Colloid Interface Sci* 1988;121.
- [48] Ramachandran V, Fogler HS. *Langmuir* 1998;14.
- [49] Ramachandran V, Fogler HS. *J Fluid Mech* 1999;385.
- [50] Kim MM, Zydney AL. *J Colloid Interface Sci* 2004;269:425–31.
- [51] Kim MM, Zydney AL. *Chem Eng Sci* 2005;60:4073–82.
- [52] Ramachandran V, Venkatesan R, Tryggvason G, Fogler HS. *J Colloid Interface Sci* 2000;229.
- [53] Vitthal S, Sharma MM. *J Colloid Interface Sci* 1995;153.
- [54] Frey JM, Schmitz P. *Chem Eng Sci* 2000;55.
- [55] Kuiper S, van Rijn CJM, Nijdam W, Krijnen GJM, Elwenspoek MC. *J Membr Sci* 2000;180.
- [56] Lin J, Bourrier D, Dilhan M, Duru P. *Phys Fluids* 2009;21.
- [57] Wyss HM, Blair DL, Morris JF, Stone HA, Weitz DA. *Phys Rev E* 2006;74.
- [58] Chen JC, Li Q, Elimelech M. *Adv Colloid Interface Sci* 2004;107:83–108.
- [59] Kuiper S, van Rijn CJM, Nijdam W, Elwenspoek MC. *J Membr Sci* 1998;150:1–8.
- [60] Brans G, van Dinther A, Odum B, Schroën CGPH, Boom RM. *J Membr Sci* 2007;290:230–40.
- [61] Vogelaar L, Lammertink RGH, Barsema JN, Nijdam W, Bolhuis-Versteeg LAM, van Rijn CJM, et al. *Small* 2005;1:645–55.
- [62] Groisman A, Lobo C, Cho H, Campbell JK, Dufour YS, Stevens AM, et al. *Nat Meth* 2005;2:685–9.
- [63] Chen X, Cui DF, Liu CC, Li H. *Sens Actuators B* 2008;130:216–21.
- [64] Mc Donald JC, Duffy DC, Anderson JR, Chiu DT, Wu H, Schueller OJA, et al. *Electrophoresis* 2000;21:27–40.
- [65] van Oss CJ. *Interfacial forces in aqueous media*. Marcel Dekker; 1994.
- [66] He Q, Liu Z, Xiao P, Liang R, He N, Lu Z. *Langmuir* 2003;19:6982–6.
- [67] Lee JN, Park C, Whitesides GM. *Anal Chem* 2003;75:6544–54.
- [68] Klammer I, Hofmann MC, Buchenauer A, Mokwa W, Schnakenberg U. *J Micromech Microeng* 2006;16:2425–8.
- [69] Adamczyk Z. *Adv Colloid Interface Sci* 2003;100:267–347.
- [70] Sharp KV, Adrian RJ. *Microfluid Nanofluid* 2005;1:376–80.